EPR and Electronic Spectra of (3-Chloroanilinium)$_8$[$CuCl_6$]Cl_4: Evidence for Tetragonally Elongated $CuCl_6^{4-}$ Ions with the Long Axis Disordered in 2-Dimensions

Horst Stratemeier,[†] Burghard Wagner,[‡] Elmars R. Krausz,[§] Rolf Linder,[∥] Hans-Herbert Schmidtke,[∥] Jürgen Pebler,[‡] William E. Hatfield,[⊥] Leo ter Haar,[#] Dirk Reinen,*[,‡] and Michael A. Hitchman*[,†]

Chemistry Department, University of Tasmania, Box 252C, Hobart, Tasmania 7000, Australia, Fachbereich Chemie, Philipps Universität, Hans-Meerwein Strasse, D-35032 Marburg/Lahn, Germany, Research School of Chemistry, Australian National University, ANU 0200, Canberra, ACT 2601, Australia, Institut für Theoretische Chemie, Heinrich-Heine-Universität Düsseldorf, Universitätsstrasse 1, D-4000 Düsseldorf 1, Germany, Chemistry Department, University of North Carolina at Chapel Hill, Chapel Hill, North Carolina 27599-3290, and Chemistry Department, University of Texas, El Paso, Texas 79968-0513

Received October 15, 1993[⊗]

The low-temperature electronic and electron paramagnetic resonance spectra of (3-chloroanilinium)$_8$[$CuCl_6$]Cl_4 suggest that at the local level each $CuCl_6^{4-}$ ion has a tetragonally elongated octahedral coordination geometry, with a significant orthorhombic distortion, rather than the tetragonally compressed geometry suggested previously. However, the directions of the long and intermediate Cu–Cl bonds are disordered, so that the bond lengths averaged over the unit cell correspond to a compressed tetragonal geometry. Magnetic susceptibility measurements suggest coupling parameters similar to those reported previously, with weak antiferromagnetic interactions in the direction parallel to the shortest Cu–Cl bond direction, and very weak ferromagnetic coupling in the plane normal to this direction, and it is shown that this is consistent with the proposed disorder in the compound. A model describing the potential surface and vibronic energy levels of the $CuCl_6^{4-}$ ion in terms of Jahn–Teller coupling and lattice strain interactions is presented, and correlated with the spectroscopic data and Cu–Cl bond lengths derived from the X-ray thermal ellipsoids.

Introduction

The Jahn–Teller theorem predicts that a regular octahedral geometry is unstable for 6-coordinate copper(II) complexes, and indeed these are invariably observed to distort away from O_h symmetry.[1] Although tetragonally elongated and compressed arrangements of the ligands are equally consistent with the theorem, the sense of the distortion is almost always to produce the former, with various factors apparently combining to cause this discrimination.[1a,2] Experimentally, it has sometimes proved difficult to distinguish between the two geometries, because a complex which has an elongated tetragonal geometry at the local level sometimes crystallizes with the long metal–ligand bonds distributed in a nonparallel manner in the overall crystal lattice. The X-ray diffraction analysis of such an—in the case of a canting angle of 90°—"antiferrodistortive" order pattern may show a directionally averaged geometry with two short and four longer metal–ligand bonds, implying a tetragonally compressed geometry. The compounds K_2CuF_4 and Ba_2CuF_6 are examples of systems which were originally misinterpreted in this way.[3,4] For K_2CuF_4, for instance, an early X-ray analysis[3] showed two Cu–F bonds of 1.95 Å and four of 2.08 Å and this has often been cited as an example of a Cu(II) complex with a compressed tetragonal geometry. However, later work[5] showed that the compound contains CuF_6^{4-} units with Cu–F bond lengths of 1.93, 1.94, and 2.22 Å, with the long bonds of neighboring CuF_6^{4-} polyhedra being perpendicularly oriented in the (001) lattice plane. Electron paramagnetic resonance (EPR) spectroscopy may also be used to characterize the geometry, since with elongated tetragonal bonds the unpaired electron is in the $d_{x^2-y^2}$ orbital, while with a compressed tetragonal geometry it occupies the d_{z^2} orbital. The two situations give rise to quite different **g** tensors. For instance, the tetragonally elongated $CuCl_6^{4-}$ complex in (cyclamH_4) $CuCl_6$ (cyclam = 1,4,8,11-tetraazacyclotetradecane) exhibits the values $g_z = 2.27$ and $g_{xy} = 2.05$,[6] while the tetragonally compressed CuF_6^{4-} complex formed when Cu^{2+} is doped into Ba_2ZnF_6 has the values[7] $g_z = 1.99$, $g_{xy} = 2.34$ in accordance with the expected **g** tensor components for an elongated (eq 1) and compressed (eq 2) geometry. Here, ξ_0 (=830 cm^{-1}) is the free-ion spin–orbit

$$g_z = g_0 + 8u_z - u_z^2 - 3u_zu_{xy} - 3u_{xy}^2;\ g_{x,y} = g_0 + 2u_{xy} - 4u_z^2$$

$$u_z = k_z^2\xi_0/E(x^2 - y^2 \rightarrow xy);\ u_{xy} = k_{xy}^2\xi_0/E(x^2 - y^2 \rightarrow xz, yz) \quad (1)$$

$$[u_z > u_{xy} \text{ and } (g_z - g_0)/(g_{xy} - g_0) > 4]$$

$$g_z = g_0 - 3v_z^2 + 3v_zv_{xy} - 3v_{xy}^2;\ g_{xy} = g_0 + 6v_{xy} - 6v_{xy}^2$$

$$v_z = k'^2_z\xi_0/E(z^2 \rightarrow xy);\ v_{xy} = k'^2_{xy}\xi_0/E(z^2 \rightarrow xz, yz) \quad (2)$$

$$[v_z < v_{xy}]$$

coupling constant of Cu^{2+}, the k_i are covalency (orbital reduction) factors and the energies are those of the respective transitions in the ligand field spectra. An identification of the sense of the

[†] University of Tasmania.
[‡] Philipps University.
[§] Australian National University.
[∥] Heinrich-Heine-Universität Düsseldorf.
[⊥] University of North Carolina at Chapel Hill.
[#] University of Texas, El Paso.
[⊗] Abstract published in *Advance ACS Abstracts,* April 15, 1994.

(1) (a) For a recent review of the Jahn–Teller effect see Reinen, D.; Atanasov, M. *Magn. Reson. Rev.* **1991**, *15*, 167. (b) For a general discussion of the influence of the Jahn–Teller effect on copper(II) chemistry see: Hathaway, B. J. *Struct. Bonding* **1984**, *57*, 55. Hathaway, B. J. *Comprehensive Coordination Chemistry*, Wilkinson, G., Ed., Pergamon: Oxford, England, 1988; Vol. 5, pp 662, 665, 698.
(2) Deeth, R. J.; Hitchman, M. A. *Inorg. Chem.* **1986**, *25*, 1225.
(3) Knox, K. *J. Chem. Phys.* **1959**, *30*, 991.
(4) von Schnering, H. G. *Z. Anorg. Allg. Chem.* **1967**, *353*, 1 and 13.
(5) Friebel, C.; Reinen, D. *Z. Anorg. Allg. Chem.* **1974**, *407*, 193. Hidaka, M.; Inoue, K.; Yamada, I. *J. Phys.* **1983**, *121B*, 343 and references therein.

0020-1669/94/1333-2320$04.50/0

distortion is not always unambiguous. Thus, an X-ray diffraction study of γ-$Cs_2PbCu(NO_2)_6$ (low-temperature phase) was interpreted as showing that the $Cu(NO_2)_6^{4-}$ entities have tetragonally compressed geometries.[8] The EPR spectrum showed a g value of 2.06 parallel to the short Cu–N bonds, and 2.15 in the plane perpendicular to this, and it was suggested[9] that this was consistent with a tetragonally compressed complex. The significant deviation of the former g value from the expected value of ~2 (eq 2) was explained in terms of an admixture of $d_{x^2-y^2}$ into the d_{z^2} ground state by vibronic coupling. Subsequent work[10] showed that the apparent compressed tetragonal geometry γ-$Cs_2PbCu(NO_2)_6$ is due to a slightly disturbed antiferrodistortive pattern of elongated polyhedra (with an orthorhombic symmetry component), similar to that in K_2CuF_4. Since electron exchange between the $Cu(NO_2)_6^{4-}$ ions in the two orientations is more rapid than the EPR timescale, the observed g values are averaged according to eq 3.[11,12] If the local geometry is tetragonal ($g_x = g_y$) the canting

$$g_x^{ex} = g_x$$

$$g_y^{ex} = (\sin^2 \alpha)g_z + (\cos^2 \alpha)g_y \qquad (3)$$

$$g_z^{ex} = (\cos^2 \alpha)g_z + (\sin^2 \alpha)g_y$$

can easily be calculated as shown in eq 3a.

$$\cos 2\alpha = (g_y^{ex} - g_z^{ex})/(2g_x^{ex} - g_y^{ex} - g_z^{ex}) \qquad (3a)$$

The canting angle 2α between the local C_4 (or $g_\parallel$) axes is ~90° and the local g values deduced from the observed exchange coupled g tensor components (eq 3) are $g_z \approx 2.24$ and $g_{xy} \approx 2.06$—consistent with eq 1 and a tetragonally elongated octahedron.

A vibronic coupling mechanism does, however, seem to be responsible for the $g_\parallel$ shift of the compressed tetragonal CuF_6^{4-} complex formed when Cu^{2+} is doped into K_2ZnF_4.[13] Here, g_z = 2.04 at room temperature, but as the influence of dynamic vibronic coupling decreases significantly on cooling, in this case g_z approaches 2.00 at 4 K, as expected (see eq 2).

Although electronic spectroscopy has not generally been applied to determine the sense of the distortion in Cu(II) complexes, the low-temperature single-crystal spectrum was used[14] to confirm the presence of tetragonally compressed CuF_6^{4-} octahedra in $KAlCuF_6$, which as far as we are aware is the only nondiluted copper(II) compound involving just one type of ligand known to have this geometry.[15] This technique thus also has the potential to aid the determination of the geometry of Jahn–Teller distorted systems.

Recently, the preparation and properties of (3-Cl-an)$_8$[CuCl$_6$]Cl$_4$ (3-Cl-an = 3-chloroanilinium) was reported.[16] The crystal structure showed the presence of isolated, centrosymmetric $CuCl_6^{4-}$ ions with two Cu–Cl bonds significantly shorter than the other four, and the EPR spectrum gave the g values 2.06 and 2.19 parallel and perpendicular to the short bonds, respectively. These results were interpreted as showing that the complex has a compressed tetragonal geometry, with the relatively high value of the former g value being caused by vibronic admixture of $d_{x^2-y^2}$ into the predominantly d_{z^2} ground state. An alternative hypothesis is that tetragonally elongated $CuCl_6^{4-}$ complexes occur, with the long and one short Cu–Cl bonds disordered throughout the lattice. Possibly this disorder may be dynamic at higher temperatures. These two possibilities are illustrated schematically in Figure 1.

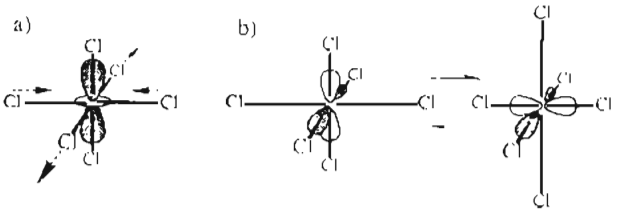

Figure 1. Schematic diagram illustrating possible models for the $CuCl_6^{4-}$ polyhedron in (3-Cl-an)$_8$CuCl$_6$]Cl$_4$: (a) a compressed tetragonal octahedral geometry and a d_{z^2} ground state; the active vibration inducing an admixture of $d_{x^2-y^2}$ by vibronic coupling is indicated by arrows; (b) an elongated tetragonal octahedral geometry with a $d_{x^2-y^2}$ ground state, with the long and one short Cu–Cl bond disordered. The antiferrodistortive arrangement illustrated probably only occurs over short distances in the lattice and may be dynamic at higher temperatures as indicated by the half-arrows.

As outlined above, the temperature dependence of the g tensor components, and the single-crystal optical spectrum should provide tests of these proposals, and we have therefore measured these properties, which support the latter, disorder model. Magnetic susceptibility measurements have also been made which essentially confirm those reported previously.[16] The potential surface of the complex is discussed in terms of a model developed[7,13,17,18] to describe a Cu(II) complex subjected to Jahn–Teller coupling and lattice strain. The implications of the new description on the magnetic properties of the compound are also considered.

Experimental Section

The preparation and characterization of single crystals of (3-Cl-an)$_8$[CuCl$_6$]Cl$_4$ has been described previously.[16] EPR spectra were measured using a Bruker ESP-300E spectrometer operating at X- and Q-band frequencies, with the sample cooled using an Oxford instruments flow cryostat. Electronic reflection spectra were recorded against sintered MgO using a Zeiss PMQ II spectrophotometer. Single-crystal electronic spectra were measured for the (010) crystal face with the electric vector parallel to the two extinction directions. Two different custom-built spectrophotometers were used to record the spectra at temperatures between 5 and 298 K. Similar results were obtained with the two instruments, and details of that used to obtain the spectra shown in Figure 5 have been described elsewhere.[19] Magnetic susceptibility data were collected between 4 and 150 K with a SQUID magnetometer.

Results and Discussion

Structural Results. The triclinic unit cell of (3-Cl-an)$_8$[CuCl$_6$]Cl$_4$ [a = 8.55 Å, b = 13.96 Å, c = 14.27 Å; α = 90.5°, β = 107.8°, γ = 102.1°] contains one isolated $CuCl_6^{4-}$ complex, with the metal on an inversion center and all ClCuCl bond angles close to 90°.[16] The bond lengths Cu–Cl(1) = 2.277 Å, Cu–Cl(2) = 2.606 Å, Cu–Cl(3) = 2.609 Å imply a tetragonally compressed geometry, with the short Cu–Cl(1) spacings being oriented almost exactly parallel to the a-axis. However, the four more distant chloride ions exhibit ellipsoids of thermal motion which are highly elongated approximately along the bond vectors (Table 1) while the ellipsoids of Cu^{2+} and the two more closely bound Cl^- ligands

(6) McDonald, R. G.; Hitchman, M. A. *Inorg. Chem.* **1989**, *28*, 3996.
(7) Steffen, G.; Reinen, D.; Stratemeier, H.; Riley, M. J.; Hitchman, M. A.; Matthies, H.E.; Recker, K.; Wallrafen, F.; Niklas, J. R. *Inorg. Chem.* **1990**, *29*, 2123.
(8) Harrowfield, B. V.; Pilbrow, J. R. *J. Phys. C.: Solid State Phys.* **1973**, *6*, 755.
(9) Harrowfield, B. V. *Solid State Commun.* **1976**, *19*, 983.
(10) Reinen, D. *Solid State Commun.* **1977**, *21*, 137. Klein, S.; Reinen, D. *J. Solid State Chem.* **1978**, *25*, 295. Klein, S.; Reinen, D. *J. Solid State Chem.* **1980**, *32*, 311.
(11) Chao, C. *J. Magn. Reson.* **1973**, *10*, 1.
(12) Reinen, D.; Dance, J.-M. *Inorg. Solid Fluorides* **1985**, *18*, 525. Reinen, D.; Krause, S. *Inorg. Chem.* **1981**, *20*, 2750.
(13) Riley, M. J.; Hitchman, M. A.; Reinen, D. *Chem. Phys.* **1986**, *102*, 11.
(14) Finnie, K.; Dubicki, L.; Krausz, E. R.; Riley, M. J. *Inorg. Chem.* **1990**, *29*, 3908.
(15) Wingefeld, G.; Hoppe, R. *Z. Anorg. Allg. Chem.* **1984**, *516*, 223.
(16) (a) Tucker, D.; White, P. S.; Trojan, K. L.; Kirk, M. L.; Hatfield, W. E. *Inorg. Chem.* **1991**, *30*, 823. (b) Hatfield, W. E.; Trojan, K. L.; White, P. S.; Horner, O.; ter Haar, L. W.; Nelson, D. J.; Cervantes-Lee, F.; Hoffmann, S. K.; Hilczer, W.; Gosler, J.; Hitchman, M. A. *Mol. Cryst. Liq. Cryst.* **1993**, *233*, 309.
(17) Riley, M. J.; Hitchman, M. A.; Reinen, D. *Inorg. Chem.* **1988**, *27*, 1924.
(18) Riley, M. J.; Hitchman, M. A.; Mohammed, A. W. *J. Chem. Phys.* **1987**, *87*, 3766.
(19) Krausz, E. R. *Aust. J. Chem.* **1993**, *46*, 1041.

Table 1. Thermal Parameters U_i (Å^2 × 10^4) of the Cu^{2+} and Cl^- Ions Constituting the $CuCl_6^{4-}$ Complex in (3-Cl-an)$_8$[$CuCl_6$]Cl_4[21]

	U_1	U_2	U_3
Cu	316	351	391
Cl(1)	318	354	381
Cl(2)	398	415	915
Cl(3)	400	450	941

are smaller and spherically symmetrical. The highly elongated ellipsoids of the more distant chlorides indicate either a low-energy Cu–Cl stretching vibration involving just these atoms, suggesting vibronic coupling effects of the kind found for Cu^{2+}-doped K_2ZnF_4, or a static or dynamic disorder of the Cl atoms along these bond directions. If the latter is correct, the approximate positions of the atoms may be estimated from the dimensions of the thermal ellipsoids.[20]

The mean square amplitude of an atom may be written[20] as the sum of a contribution due to vibrations U_{vib} and a contribution U_{dis} caused by the displacement of the disordered atoms from their mean position:

$$U = U_{vib} + U_{dis} \quad (4)$$

Substituting in eq 4 the value $U_3 \approx 930 \times 10^{-4}$ Å^2 for Cl(2) and Cl(3),[21] which is correlated approximately with the Cu–Cl(2,3) bond directions, and taking for U_{vib} the value observed for the non-disordered Cl(1), $U_{vib} \approx 380 \times 10^{-4}$ Å^2,[21] yields the estimate $U_{dis} \approx 550 \times 10^{-4}$ Å^2 for the contribution of the disorder to the thermal ellipsoids of Cl(2) and Cl(3). This corresponds to a displacement of the disordered atoms from the mean position by $U_{dis}^{1/2} \approx 0.24$ Å and implies that the *apparent* bond length of 2.61 Å to atoms Cl(2) and Cl(3) is in fact due to a disorder of bonds of length 2.61 ± 0.24 Å, leading to an elongated octahedral geometry with an orthorhombic symmetry component. The Cu–Cl spacings are 2.28, ~2.37, and ~2.85 Å, with the shortest bond always to Cl(1) and an essentially equal number of complexes having the latter two bond lengths correlated with Cu–Cl(2) and Cu–Cl(3) and Cu–Cl(3), and Cu–Cl(2), respectively.

The above model thus suggests that the apparent compressed tetragonal geometry of the $CuCl_6^{4-}$ group in (3-Cl-an)$_8$[$CuCl_6$]-Cl_4 is due to a 2-dimensional arrangement of alternating long and intermediate bonds. The disorder may be static or fluxional, and we will discuss this point below. The axial spacings are somewhat shorter than those[22] of the isolated $CuCl_6^{4-}$ ions in (cyclamH_4)$CuCl_6$ (Cu–Cl = 2.29, 2.30, and 3.18 Å), but quite similar to those in several compounds in which chlorides link copper(II) ions via long and short bonds;[23] *e.g.* Cu–Cl = 2.28, 2.36, and 2.78 Å in $CsCuCl_3$[24] and 2.28, 2.29, and 2.98 Å in $[(C_2H_5)NH_3]_2CuCl_4$.[25] It is noteworthy that the atoms of the chloroanilinium cation which are closest to Cl(2) and Cl(3) also have rather large thermal ellipsoids,[21] suggesting that some change in orientation of the counterion accompanies the proposed interchange of the Cu–Cl bond lengths. Preliminary results from X-ray crystal structure analyses at 150 and 110 K[16b] suggest that the structure does not alter significantly on cooling to these temperatures. In particular, the anisotropies of the thermal ellipsoids of Cl(2) and Cl(3) at 150 K are very similar to those at room temperature,[26] which is consistent with disorder in the position of these atoms, rather than a low-energy vibrational mode.

EPR Spectra and Magnetic Properties. The EPR powder spectra of (3-Cl-an)$_8$[$CuCl_6$]Cl_4 (Q- and X-band) were measured at temperatures between 293 K and 3.7 K, and single-crystal spectra (Q-band) were recorded at 293 and 4.2 K.

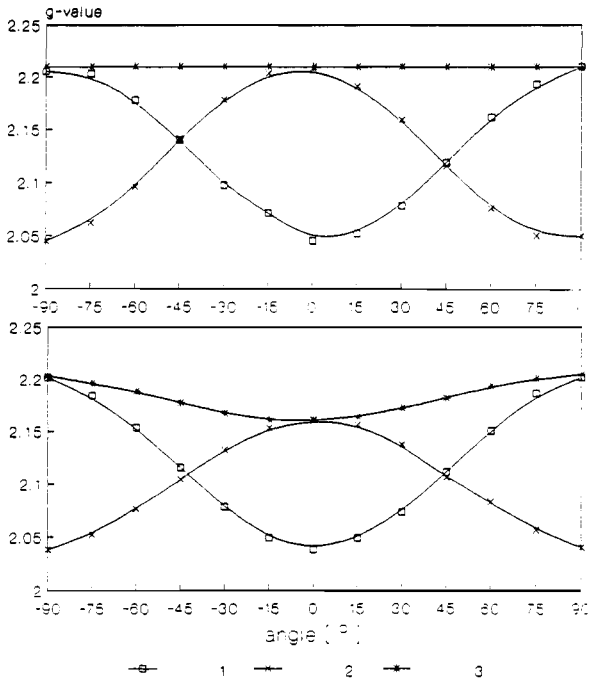

Figure 2. Angular dependence of the g values of (3-Cl-an)$_8$$CuCl_6$]$Cl_4$ (Q-band) at 298 K (above) and 4 K (below). 1, 2, and 3 refer to the plane perpendicular to a and the two planes orthogonal to each other and to 1.

Typical plots of the variation of the g values for rotations of the magnetic field in the plane perpendicular to the a-axis of the needle shaped crystals and the two orthogonal planes containing the a-axis are shown in Figure 2. The **g** tensor has axial symmetry at 293 K, with $g_x = 2.04_5$ (x is defined along the Cu–Cl(1) direction) and $g_{yz} = 2.20_1$, values reasonably close to those reported previously ($g_x = 2.06$, $g_{yz} = 2.19$).[16] The angular dependence of the **g** tensor components at 293 K shows that g_x follows the Cu–Cl(1) direction and g_{yz} correlates with the Cu–Cl spacings in the (100) plane. At 4 K an orthorhombic component appears, with g values in the (100) plane of $g_z = 2.20_5$ and $g_y = 2.16_5$.

The temperature dependence of the powder Q- and X-band spectra essentially confirm these results. The orthorhombic splitting is not resolved at X-band, but is clearly seen in the Q-band g_{yz} signal below about 10 K. While g_x remains constant within 2.040 ± 0.005 on cooling, g_{yz} decreases from 2.20_3 to 2.18_9. The former result argues strongly against the complex having a tetragonally compressed geometry, because a positive deviation of g_x from g_0 will then be due to a vibronic admixture of $d_{x^2-y^2}$ into the d_{z^2} ground state, and this should decrease substantially on cooling. This aspect is discussed below.

The EPR results thus suggest that, at least at very low temperature, locally elongated $CuCl_6^{4-}$ polyhedra occur (with a distinct orthorhombic distortion component), with the long axes being oriented alternatively along the Cu–Cl(2) and Cu–Cl(3) bonds. The orthorhombic symmetry component, which appears below 10 K, can be explained either by the presence of a very small orthorhombic lattice strain, or by exchange coupling with a canting angle $2\alpha \neq 90$ (eq 3). We prefer the first alternative, because the magnitude of the orthorhombic component in the g_{yz} signal seems to depend on temperature.

On cooling below ~9 K, satellite lines develop in the powder spectra at higher and lower field than the resonances observed above this temperature (Figure 3). The temperature dependent shifts in field are apparently identical at X- and Q-band frequencies. Similar satellite spectra were observed in the low-temperature EPR spectrum of K_2CuF_4 and Ba_2CuF_6, and these were interpreted[12] in terms of internal magnetic fields associated with the long-range ferromagnetic ordering which occurs in this temperature range. For (3-Cl-an)$_8$[$CuCl_6$]Cl_4 the satellite signals

(20) Stebler, M.; Bürgi, H. *J. Am. Chem. Soc.* **1987**, *109*, 1395.
(21) Reference 16, Supplementary Figure and Table II.
(22) Studer, M.; Riesen, A.; Kaden, Th.A. *Helv. Chim. Acta* **1989**, *72*, 1253.
(23) Smith, D. W. *Coord. Chem. Rev.* **1976**, *21*, 93.
(24) McGinnety, J. A. *J. Am. Chem. Soc.* **1972**, *94*, 8406.
(25) Steadman, J. P.; Willett, R.D. *Inorg. Chim. Acta* **1970**, *4*, 367.
(26) ter Haar, L.; Cervantes-Lee, F. Private communication..

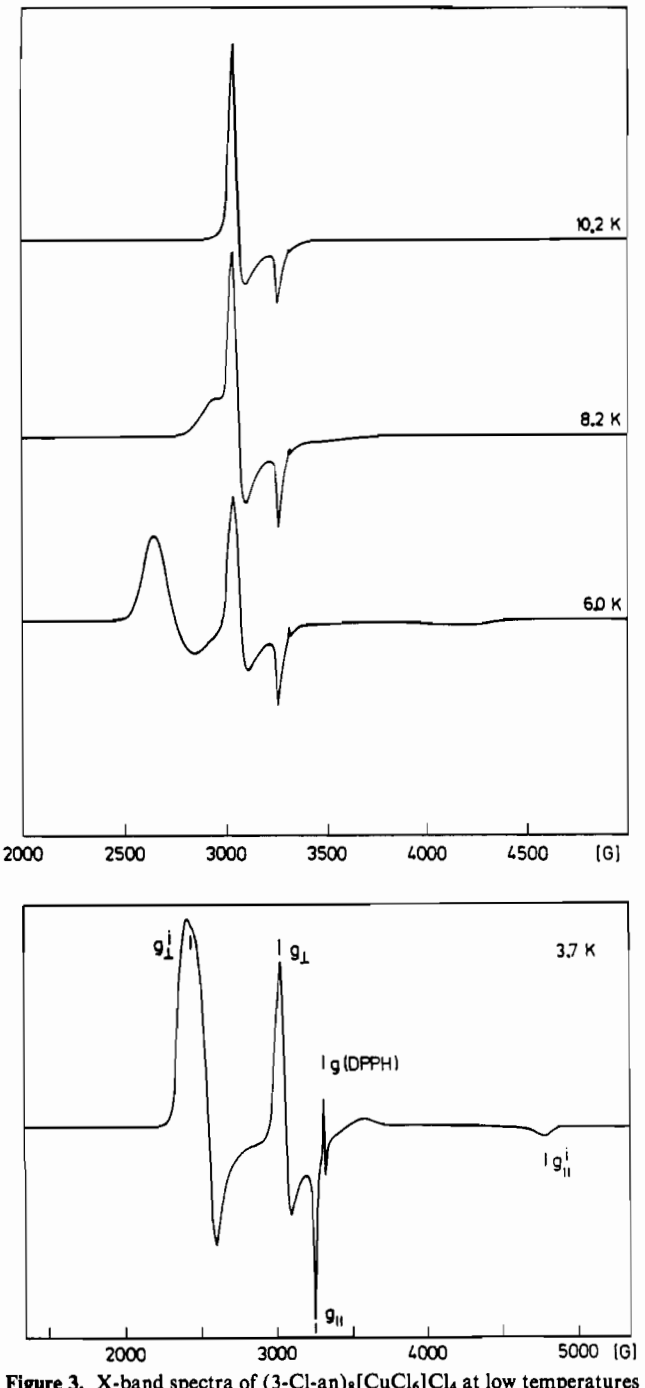

Figure 3. X-band spectra of (3-Cl-an)$_8$[CuCl$_6$]Cl$_4$ at low temperatures with satellite lines developing below ~9 K. The latter signals (g^i), probably generated by magnetic ordering, are fully resolved at 3.7 K.

develop gradually as the temperature is lowered below 9 K, but never entirely replace the primary signals, at least down to 3.7 K, as happens in the cited cases. At 3.7 K the signal associated with g_y, g_z is shifted ~600 G to lower fields, with an orthorhombic splitting occurring, as in the primary signal, while the considerably weaker one associated with g_x occurs at ~1500 G higher field. If this interpretation is correct, long-range magnetic ordering is still incomplete at 3.7 K. It also implies that an internal field of about −1500 G is generated at each Cu^{2+} when the external field is parallel to the *a* axis, and ~600 G when the external field is in the plane normal to this direction. As yet, we have been unable to resolve the satellite lines in the spectra of single-crystals. Presumably the additional spectrum is too weak in this case, because the satellite signals usually split into a broad range of separate lines at each orientation,[12] thus widely distributing the total intensity. The study of the orientation and temperature dependence of the satellite lines would appear to offer a novel method of probing the internal magnetic fields generated in magnetically ordered systems, and we intend to investigate this aspect of the spectra further.

Magnetic susceptibility data were collected between 4 and 295 K (Figure 4) and could be fitted using a linear Heisenberg $S = {}^1/_2$ chain theory (Bonner–Fisher model).[27] This basically confirms the analysis given in ref 16a, and suggests a calculated isotropic exchange energy $J = -6.2(2)$ cm^{-1} (for $g = 2.0$) similar to that obtained previously ($J = -5.6$ cm^{-1}). The broad maximum of χ_m at 11.4 K marks the temperature at which the one-dimensional correlations break down. The $kT(\chi_{max})/|J|$ ratio of 1.281 is very near to the predicted theoretical value (1.282). From the extrapolation of χ_m between 250 and 40 K we obtained a Θ_p temperature of −5.8 K and by fitting to the Curie-Weiss law a constant C of 0.346(5) cm^3 K/mol and an effective magnetic moment of 1.66(5) μ_B, which is slightly smaller than the spin-only value of 1.73 μ_B. We observed a small field dependence of the susceptibility below $T \approx 3$ K which seems to be connected with the minimum in the $\chi_m - T$ curve at 2.8 K and indicates a ferromagnetic component to the ordering. The reason is presumably a canting of the otherwise antiferromagnetically ordered spins within the chains parallel to *a*, which only becomes apparent upon 3-dimensional magnetic ordering due to interchain coupling. The exchange integral J' for the 3-dimensional order (Heisenberg model) below $T_N = 2.8(5)$ can be calculated by using the relationship[28]

$$kT_N/|J| = [2S(S+1)]^{1/2}R^{1/2} \qquad (5)$$

with $R = |J'/J|$, yielding $|J'| = 0.54(5)$ cm^{-1}, a somewhat smaller value than that estimated previously (2.1 cm^{-1}).[16a] While the linear chain consists of Cu^{2+} ions separated by 8.55 Å along the crystallographic *a*-axis, the interchain interaction involves Cu^{2+}–Cu^{2+} spacings of ~14 Å. Applying the theory of Oguchi[29] an even smaller interchain exchange constant $|J'| = 0.15(5)$ cm^{-1} is obtained. The satellite lines observed in the EPR spectra below about ~9 K are presumably due to the one-dimensional correlations within the Cu^{2+} chains along the *a*-axis. The observation that these lines shift with decreasing temperature due to increasing internal magnetic fields is also in accord with a linear chain magnetism.

Although the magnetic results cannot be used to distinguish unambiguously between the alternative structural models for (3-Cl-an)$_8$[CuCl$_6$]Cl$_4$, because the nature of the superexchange pathway is not clear, the disorder model appears to be in better accord with the data. Overlap between half-filled orbitals (either direct or by superexchange) produces antiferromagnetic coupling, while when the interaction occurs between half-filled orbitals which are orthogonal, this causes ferromagnetic coupling. The disorder model suggests that at low temperature the $CuCl_6^{4-}$ groups probably occur in domains with the long and short axes in the (100) plane alternating in an antiferrodistortive manner (Figure 1b). In this plane the lobes of the half-filled d-orbitals on neighboring ions are therefore orthogonal, which is consistent with weak ferromagnetic coupling, as observed. The compound K_2CuF_4 has an identical arrangement, except that the metal ions are linked by bridging ligands, so that the Cu^{2+}–Cu^{2+} distances are shorter and a stronger ferromagnetic interaction is indeed observed.[30] If the $CuCl_6^{4-}$ groups did have a true tetragonally compressed octahedral geometry, the in-plane circular lobe of the half-filled d_{z^2} orbital would be directed at each chloride ion in the (100) plane (Figure 1a) so that a very weak antiferromagnetic interaction might be expected in this plane, in contrast

(27) Bonner, J. C.; Fisher, M. E. *Phys. Rev.* **1964**, *A135*, 640.
(28) Mennenga, G.; de Jongh, L. J.; Huiskamp, W. J.; Reedijk, J. *J. Magn. Mater.* **1984**, *44*, 89.
(29) Oguchi, T. *Phys. Rev.* **1964**, *A133*, 1098.
(30) Reinen, D.; Friebel, C. *Struct. Bonding* **1979**, *37*, 1.

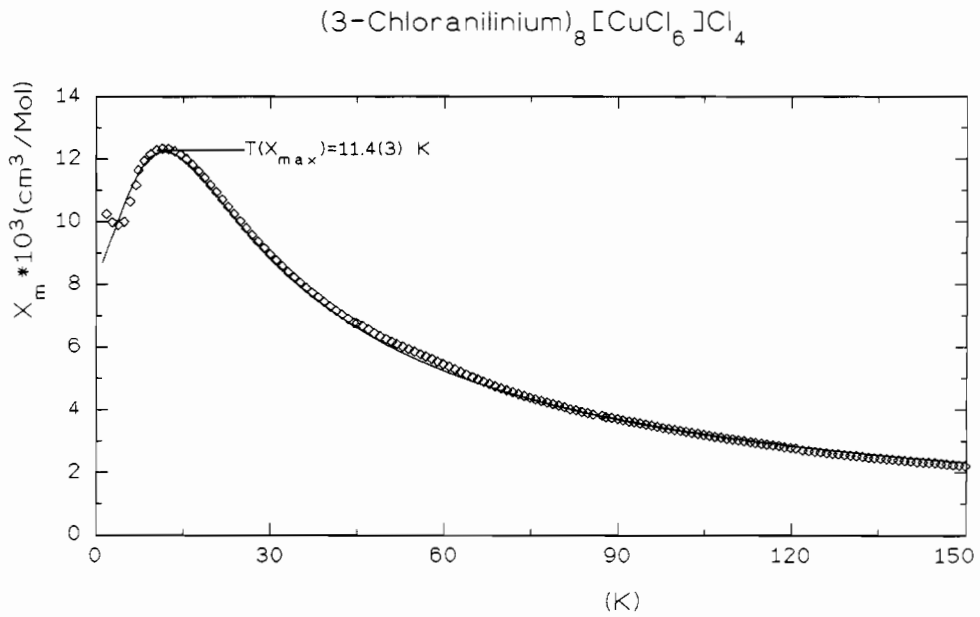

Figure 4. Plot of the molar magnetic susceptibility data of (3-Cl-an)$_8$[CuCl$_6$]Cl$_4$ against temperature. The solid line represents the best fit using a Heisenberg antiferromagnetic chain model [magnetic field = 30 kG; g = 2.0; S = $^1/_2$; J/k = −6.2 cm^{-1}].

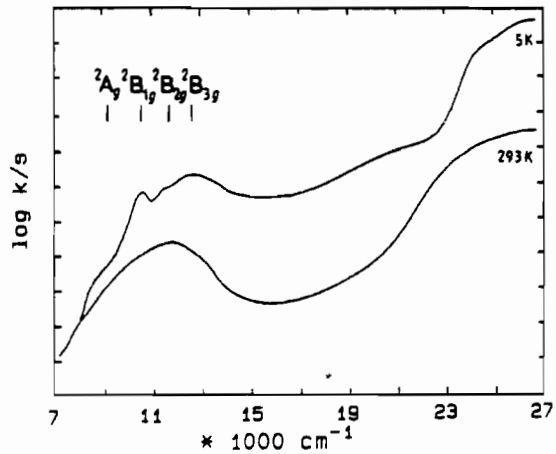

Figure 5. Powder reflection spectrum of (3-Cl-an)$_8$[CuCl$_6$]Cl$_4$ measured at 5 and 293 K. Assignment is as discussed in the text.

to the experimental findings. Both models imply that the Cu–Cl bonds parallel to the *a*-axis involve half-filled d-orbital lobes, implying modest antiferromagnetic coupling in this direction, as is indeed observed.

Electronic Spectrum. The reflectance spectra of (3-Cl-an)$_8$-[CuCl$_6$]Cl$_4$ at 293 K and 5 K are shown in Figure 5. The low-temperature spectrum shows a band centered at 12 700 cm^{-1} with a further peak at 10 400 cm^{-1} and shoulders at ~11 500 cm^{-1} and ~9000 cm^{-1}. The high- and low-temperature spectra of the (010) face of the compound were also measured using polarized light, and typical spectra with the electric vector of light along the extinction directions approximately parallel (∥) and perpendicular (⊥) to the *a* crystal axis are shown in Figure 6. The extinction coefficients of the bands were estimated by measuring the thickness of the crystal, and the low values are consistent with the centrosymmetric nature of the complex; *e.g.* the bands are only vibrationally allowed. The fact that the band areas decrease somewhat when lowering the temperature is also consistent with this mechanism (Figures 5 and 6). The band maxima shift significantly to higher energy on cooling (Figure 6), a feature which has been also observed in the spectra of other chlorocuprates.[31] In both the single crystal and reflectance spectra

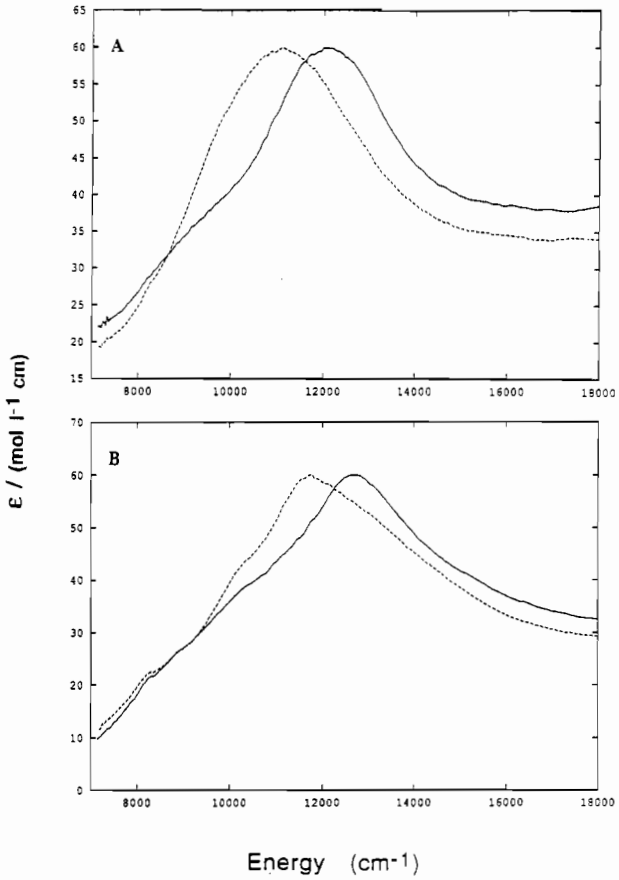

Figure 6. Spectrum of the (010) crystal face of (3-Cl-an)$_8$[CuCl$_6$]Cl$_4$ with the electric vector approximately parallel (dashed line) and perpendicular (full line) to the *a* crystal axis, measured at 293 K (A) and 5 K (B).

the background absorption increases significantly as the wavelength of the light decreases, the cause of this being unclear.

The model discussed below suggests that the CuCl$_6^{4-}$ ion in (3-Cl-an)$_8$ [CuCl$_6$]Cl$_4$ has D_{2h} symmetry. If a local axis system is defined with **x**, **y**, and **z** along the short, intermediate and long Cu–Cl bond directions, respectively, the ground state is of ^2A_g symmetry and the excited states, in probable order of increasing energy are of ^2A_g, $^2B_{1g}$, $^2B_{2g}$ and $^2B_{3g}$ symmetry. The vibronic

(31) Riley, M. J.; Hitchman, M. A. *Inorg. Chem.* **1987**, *26*, 3205 and references therein.

selection rules indicate that transitions to the latter three states are forbiden in z, y, and x polarization, respectively. Because the short Cu–Cl(1) bond is nearly parallel to the *a* crystal axis, the (‖) spectrum is almost entirely x polarized. In agreement with the selection rules, the highest energy band at ~12 700 cm^{-1} at 5 K is indeed absent in this polarization (Figure 6). The disorder model implies that in (⊥) polarization equal numbers of complexes will occur with the electric vector parallel to y and z (Figure 1b), so that the middle two transitions are expected to decrease in intensity on going from (‖) to (⊥) polarization. Indeed the band at 11 700 cm^{-1} and the shoulder at ~10 500 cm^{-1} behave in this manner. The transition to the ^2A_g state is formally allowed in each polarization, and accordingly the poorly resolved shoulder at ~9000 cm^{-1}, best seen in the spectra at 293 K, exhibits no polarization. The polarization properties of the electronic transitions thus conform well with the disorder model presented above. The alternative proposal, that the complex has a compressed tetragonal geometry of D_{4h} symmetry, would predict only three transitions (assuming, as is almost always the case, that the spin–orbit splitting of the ^2E_g state is not resolved), rather than the four which are observed experimentally.

Metal–Ligand Bonding. The angular overlap model (AOM)[32] has proved useful in the analysis of the energy levels of chlorocuprate complexes having a wide range of geometries.[33] It is thus of interest to see whether the disorder model outlined above produces chemically reasonable AOM bonding parameters for (3-Cl-an)$_8$[$CuCl_6$]Cl_4. This was investigated using the computer program CAMMAG developed by Gerloch and coworkers,[34] which has been described in detail elsewhere.[35] For a ligand such as chloride, where π-bonding is expected to be isotropic about the bond axis, the metal–ligand σ- and π-interactions are represented by the parameters e_σ and e_π, respectively. Initial estimates of the bonding parameters of the two more closely bound chlorides may be obtained from those derived already for the planar $CuCl_4^{2-}$ ion in a range of lattices,[36] with $e_\sigma \approx 5285$ cm^{-1} and $e_\pi \approx 885$ cm^{-1}, for an average Cu–Cl bond length of 2.26 Å. Assuming that the bonding parameters vary as $\sim r^{-5}$ (r being the metal–ligand bond distance) which is consistent with both theory[37] and experiment[38] for small changes in bond length, suggests bonding parameters $e_\sigma \approx 5070$ cm^{-1} and $e_\pi \approx 850$ cm^{-1} for the shortest Cu–Cl bond in (3-Cl-an)$_8$[$CuCl_6$]Cl_4, and $e_\sigma \approx 4180$ cm^{-1} and $e_\pi \approx 700$ cm^{-1} for the Cu–Cl bond of length ~2.37 Å. The parameters of the long Cu–Cl bond cannot be estimated in this way, since it has been observed[39] that the energy of the $^2A_g(z^2)$ state in complexes with large tetragonal distortions is significantly depressed in energy compared with the predictions of simple bonding theories. This has been explained either in terms of configuration interaction with the higher energy ^2A_g-(4s) state,[40] or as due to an effective interaction with the "voids" in the coordination sphere generated as the complex departs from cubic symmetry.[41] In the present case, therefore, the bonding parameters of the chloride thought to lie ~2.85 Å from copper(II) were taken to be free variables. The following bonding parameters (in cm^{-1}, for the shortest, *s*, intermediate, *i*, and longest, *l*, Cu–Cl bonds, respectively) were found to give good agreement with the experimentally observed transitions of (3-Cl-an)$_8$[$CuCl_6$]Cl_4:

$$e_\sigma^s \approx 5100,\ e_\pi^s \approx 860;\ e_\sigma^i \approx 4000,\ e_\pi^i \approx 600;$$
$$e_\sigma^l \approx 200,\ e_\pi^l \approx 100 \quad (6)$$

The calculated transition energies (in cm^{-1}, with the experimental values in parentheses) are

8800 (~9000); 10 730 (~10 500);
11 940 (11 700); 12 680 (12 700)

An effective spin–orbit coupling coefficient of 600 cm^{-1} was used in the calculation. The parameters for the longest bond compare well with those obtained by Deeth and Gerloch[42] in a study of a series of chlorocuprates of varying tetragonality. The *g* values calculated using CAMMAG

$$g_x = 2.03_6;\ g_y = 2.09_0;\ g_z = 2.30_1$$

also agree with those observed experimentally, if rapid electron exchange between $CuCl_6^{4-}$ polyhedra oriented in an antiferrodistortive pattern is assumed (Figure 1b, see following section). An isotropic orbital reduction parameter of 0.72 was used in the calculation, which is similar to the values $k_z \approx 0.71$ $k_{xy} = 0.64$ estimated[43] using perturbation methods for the tetragonally elongated $CuCl_6^{4-}$ complex in $(NH_3C_2H_5)_2CuCl_4$. Calculations were also performed assuming that the $CuCl_6^{4-}$ complex in (3-Cl-an)$_8$[$CuCl_6$]Cl_4 has a true tetragonally compressed geometry. The bonding parameters of the chlorides at 2.28 Å remain as above (e_σ^s, e_π^s), and scaling the parameters reported for planar $CuCl_4^{2-}$ ion for the differences in bond length, as described above, yields the estimates $e_\sigma \approx 2570$ cm^{-1} and $e_\pi \approx 430$ cm^{-1} for the four Cu–Cl bonds of length 2.61 Å. The calculated transition energies with respect to the $^2A_{1g}$ ground state in cm^{-1} are

5020 ($^2B_{1g}$); 9800, 10 600 (^2E_g); 11 300 ($^2B_{2g}$)

This model is unable to adequately explain the prominent peak observed at 12 700 cm^{-1} and predicts the transition between the split states of the octahedral parent ^2E_g ground state to occur at much too low an energy. The calculated (eq 2) *g* values, $g_\parallel = 1.99_0$ and $g_\perp = 2.23_7$, are also in poor agreement with those observed experimentally.

Potential Surface of the Complex Compared with Those of Other Systems. Recently, considerable progress has been made in the quantitative interpretation of the geometries and spectroscopic properties of copper(II) complexes in terms of Jahn–Teller coupling,[1,44] and it is of interest to apply these methods to the $CuCl_6^{4-}$ ion in (3-Cl-an)$_8$[$CuCl_6$]Cl_4. Conventionally, the potential surface of a complex of this type is described in terms of the coupling between the ^2E_g electronic state and the ϵ_g Jahn–Teller active vibrational mode of the parent octahedral complex. To first order, a complex with identical ligands undergoes a radial distortion in the ϵ_g mode to yield the "Mexican hat" potential surface pictured in Figure 7A. At this level of approximation, the Q_θ and Q_ϵ components of the vibration (Figure 7B) are equivalent, and the energy minimum is a circular well of radius ρ. If the position of the complex in this well is defined by an angle ϕ, the ligand coordination geometry is described by the relationships

$$Q_\theta = \rho(\cos\phi);\ Q_\epsilon = \rho(\sin\phi) \quad (7)$$

(32) Jørgenson, C. K.; Pappalardo, R.; Schmidtke, H.-H. *J. Chem. Phys.* **1963**, *39*, 1422; Schäffer, C. E. *Pure Appl. Chem.* **1970**, *24*, 361 and references therein.
(33) Hitchman, M. A.; Cassidy, P. *J. Inorg. Chem.* **1978**, *17*, 1682.
(34) Cruse, D. A.; Davies, J. E.; Gerloch, M.; Harding, J. H.; Mackey, D. J.; McMeecking, R. F. *CAMMAG, a FORTRAN Computing Package*, University Chemical Laboratory: Cambridge, England, 1979.
(35) Gerloch, M. *Magnetism and Ligand-Field Analysis*, Cambridge University Press, England, 1983.
(36) McDonald, R. G.; Hitchman, M. A. *Inorg. Chem.* **1986**, *25*, 3273.
(37) Smith, D. W. *J. Chem. Phys.* **1969**, *50*, 2784; Bermejo, M.; Pueyo, L. *J. Chem. Phys.* **1983**, *78*, 854.
(38) Drickamer, H. G.; Frank, C. W. *Electronic Transitions and the High-Pressure Chemistry and Physics of Solids;* Chapman-Hall: London, 1972.
(39) Vanquickenborne, L. G.; Ceulemans, A. *Inorg. Chem.* **1981**, *20*, 796.
(40) Smith, D. W. *Inorg. Chim. Acta* **1977**, *22*, 107.
(41) Deeth, R.J.; Gerloch, M. *Inorg. Chem.* **1984**, *23*, 3846.
(42) Deeth, R. J.; Gerloch, M. *Inorg. Chem.* **1985**, *24*, 1754.
(43) Cassidy, P. J.; Hitchman, M. A. *Inorg. Chem.* **1977**, *16*, 1568.
(44) Hitchman, M. A. *Comments Inorg. Chem.* **1994**, *15*, 197.

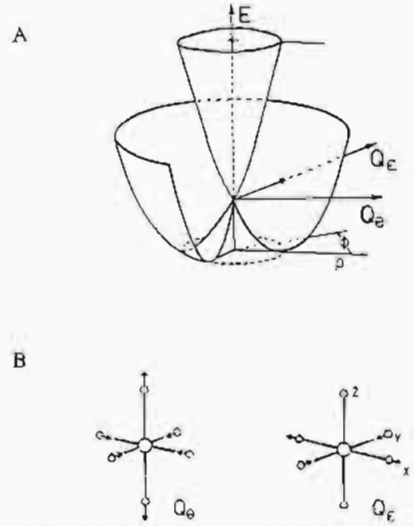

Figure 7. Mexican hat potential surface caused by linear $E_g \oplus \epsilon_g$ vibronic coupling (A) and form of the two components of the ϵ_g vibrational mode (B).

with $\rho = \{2(\delta x^2 + \delta y^2 + \delta z^2)\}^{1/2}$, where δx, δy, and δz are the deviations from the mean value of the metal–ligand bond lengths along the **x**, **y**, **z** cartesian axes. Higher order effects cause a warping of the Mexican hat potential surface to give three equivalent minima at ϕ = 0, 120, and 240°, each of which corresponds to a tetragonally elongated geometry. The appearance of the lower energy region of this warped Mexican hat potential surface is shown as a contour energy plot on the left-hand side of Figure 8a, while the energy variation of such a system as a function of ϕ, for the Jahn–Teller radius ρ of the three potential energy minima, is shown on the right. The three equivalent energy minima correspond to the long tetragonal axis lying along **z**, **y**, or **x**. Interconversion between these is possible by moving along the Q_ϵ component of the ϵ_g vibration. Thermal population of higher vibronic levels allows the saddle points which describe tetragonally compressed geometries to be surpassed. The extent of the warping is normally expressed by the parameter β, where the energy difference between the minima and saddlepoints is given by 2β. The circular plot of constant Jahn–Teller radius overestimates the energy of the saddle points which must be traversed as a complex "switches" the direction of the long tetragonal axis. As may be seen from the corresponding energy contour plot, the minimum energy pathway is more triangular than circular.

A theoretical model has been developed to desribe the electronic and geometric properties of 6-coordinate copper(II) complexes along the above lines. This approach, described in detail elsewhere,[7,13,17,18] calculates the vibronic energy levels of the complexes by applying Jahn–Teller coupling (defined by a linear coupling constant A_1), plus the "warping" interaction (second order coupling constant A_2) to a basis set consisting of the $d_{x^2-y^2}$ and d_{z^2} electronic wave functions, and about 40 harmonic oscillator wave functions of the ϵ_g vibration. The definition of the parameters is discussed in detail in ref 13. When the six ligands are not equivalent, a "strain" is added by means of axial and orthorhombic components S_θ and S_ϵ. By convention, the principal direction along which the strain acts is defined as **z**, and a positive value of S_θ cause the ligands along this axis to move out, while those along **x** and **y** approach the metal; a positive value of S_ϵ causes the bonds along **y** to contract and those along **x** to expand. The *g* values are derived from the electronic parts of the eigenfunctions of the calculation, and the temperature dependence is given by the changes in the Boltzmann populations of the energy levels. The molecular geometry associated with the vibrational part of each eigenfunction may be estimated via the relationships

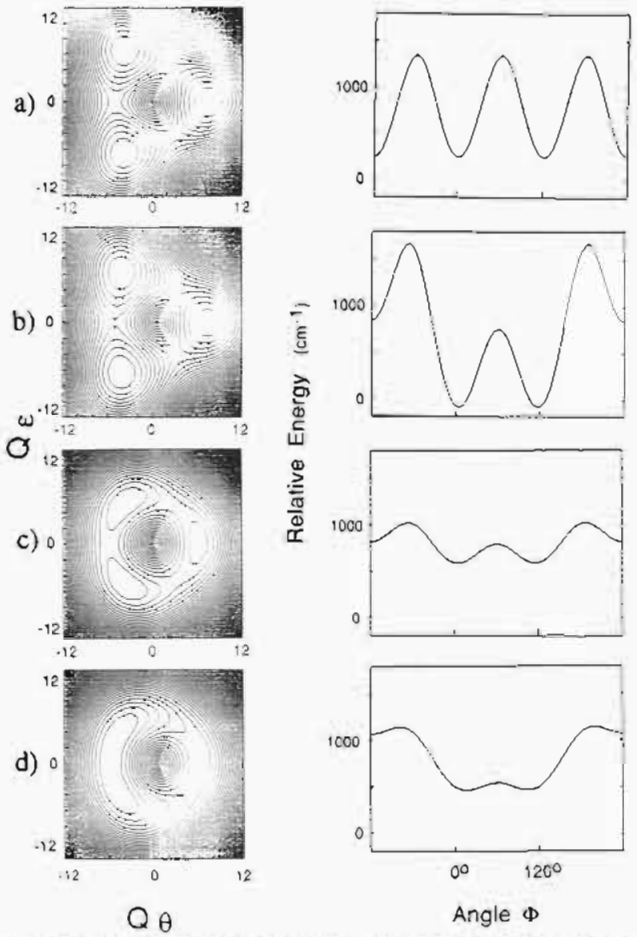

Figure 8. Lower energy region of the warped Mexican hat potential surface calculated for the $CuCl_6^{4-}$ ion for various estimates of the lattice strain parameters (left-hand side). The corresponding variation of the energy as a function of the angle ϕ, at a constant Jahn–Teller radius equal to that at the energy minimum, is shown on the right-hand side. The following parameters in reciprocal centimeters were used to define the potential surfaces (see text for definition): (a) A_1 = 900, $h\nu$ = 150, A_2 = 15.4, S_θ = 0, S_ϵ = 0; (b) A_1 = 900, $h\nu$ = 150, A_2 = 15.4, S_θ = –600, S_ϵ = 0.3; (c) A_1 = 900, $h\nu$ = 150, A_2 = 3.8, S_θ = –150, S_ϵ = 0.3; (d) A_1 = 900, $h\nu$ = 200, A_2 = 1.7, S_θ = –375, S_ϵ = 0.3.

$$\langle x \rangle = -\sqrt{(1/12)}\langle Q_\theta \rangle + (1/2)\langle Q_\epsilon \rangle$$

$$\langle y \rangle = -\sqrt{(1/12)}\langle Q_\theta \rangle - (1/2)\langle Q_\epsilon \rangle$$

$$\langle z \rangle = \sqrt{(1/3)}\langle Q_\theta \rangle \qquad (8)$$

The expectation values $\langle x \rangle$, $\langle y \rangle$ and $\langle z \rangle$ are dimensionless and can be converted into bond length changes in pm along each axis by multiplying by $0.001722(mhc\nu)^{1/2}$, where m is the ligand mass in atomic units and ν refers to the ϵ_g vibration.

In order to apply the model to $(3\text{-Cl-an})_8[CuCl_6]Cl_4$, the above parameters must be estimated for the $CuCl_6^{4-}$ ion. The linear Jahn–Teller coupling coefficient A_1 was taken to be ~900 cm^{-1}, a value previously used[17,18] in calculations on the complexes $CuCl_4(H_2O)_2^{2-}$ and $Cu(H_2O)_6^{2+}$, and of similiar magnitude to that estimated by Bacci[45] for the $CuCl_6^{4-}$ ion. Experimental data for the vibrational spectra of hexachlorocomplexes of divalent transition metals are not available. Thus the energy of the ϵ_g vibration of the $CuCl_6^{4-}$ ion cannot be derived directly. Assuming a similar force constant to that estimated[18] for $Cu(H_2O)_6^{2+}$ and correcting for the difference in ligand mass yield an energy of ~200 cm^{-1}, the value assumed by Bacci in his treatment of the Jahn–Teller coupling in the $CuCl_6^{4-}$ ion.[45] However, this leads to a Jahn–Teller radius which is too small, not only for $CuCl_6^{4-}$ in $(3\text{-Cl-an})_8[CuCl_6]Cl_4$, where ρ is estimated as ~0.61Å (eq 7)

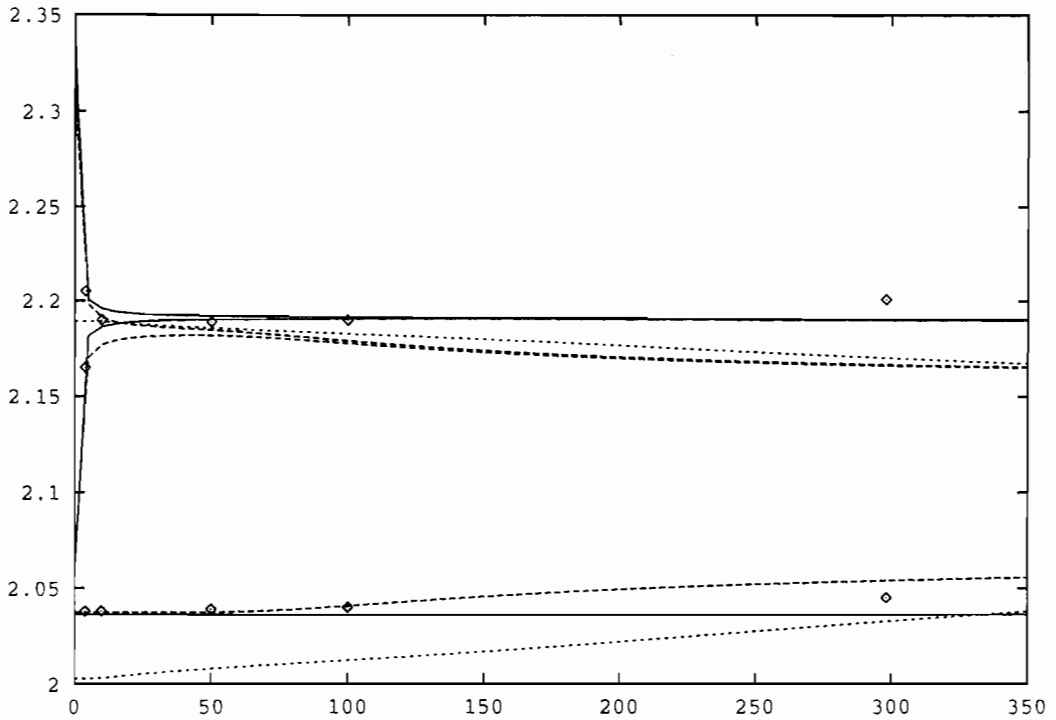

Figure 9. Calculated variation of the g values of the $CuCl_6^{4-}$ complex in (3-Cl-an)$_8$[$CuCl_6$]Cl_4 for the potential surfaces pictured in Figure 8b (full lines), Figure 8c (dashed lines) and Figure 8d (dotted lines). Selected experimental g values are also shown.

from the Cu–Cl bond lengths derived from the crystallographic thermal ellipsoids (note that to first order $\rho \approx |A_1|/k$, k being the force constant of the ϵ_g vibration), but also in other compounds containing this species.[23] Anharmonicity effects are likely to be important at long Cu–Cl distances and possibly these influence the potential surface.[2] For this reason the effective energy of the ϵ_g vibration was taken to be ~ 150 cm^{-1} in the present calculations. The warping of the potential surface is most conveniently represented in the calculation by a second order vibronic coupling coefficient A_2, which is related to the parameter β by the approximation[18]

$$\beta \approx A_2 A_1^2/(h\nu)^2 \qquad (9)$$

Estimates of β vary widely, from close to zero for Cu^{2+}-doped MgO,[46] to 50–100 cm^{-1} in doped fluoride[7,13] and NH_4Cl[17] lattices, to 300–600 cm^{-1} for the $Cu(H_2O)_6^{2+}$ ion.[18,47,48] The magnitude of the warping is apparently a balance between several competing factors,[1,2] and it has been suggested[2] that β is likely to be larger for complexes involving isolated ligands than in continuous lattices. A wide range of values of β was explored in the present calculations, and a value in the upper limits of the above range was found, this being consistent with the isolated nature of the complex in (3-Cl-an)$_8$[$CuCl_6$]Cl_4.

The contour energy plot of the lower region of the Mexican hat potential surface shown on the left side of Figure 8a is that estimated for the $CuCl_6^{4-}$ complex as it would ocur in an isotropic lattice ($A_2 = 15.4$ cm^{-1} corresponds to $\beta = 550$ cm^{-1} for $h\nu = 150$ cm^{-1}). When copper(II) is in a site of lower than cubic symmetry, the positions and relative energies of the potential energy minima are shifted in position and relative energy, due to lattice strain effects. For the $CuCl_6^{4-}$ complex in (3-Cl-an)$_8$[$CuCl_6$]Cl_4 the only crystallographic symmetry at the metal is an inversion center, so that formally both axial and orthorhombic lattice strain components, S_θ and S_ϵ must be included in the calculations. However, the fact that the **g** tensor maintains tetragonal symmetry down to very low temperature suggests that the orthorhombic component is very small. This was confirmed by estimating the potential surface and associated wave functions for a wide range of values of the strain and warping parameters, and comparing the calculated g values and molecular geometry with those observed experimentally. Clearly, the axial strain is negative, corresponding to axial compression. As noted previously,[12] under the cirumstances that $|S_\theta|$ is less than 9β, three minima occur with two of them representing orthorhombic geometries. The relative energies and positions of the minima largely depend on the ratio of $|S_\theta|$ to β, and good agreement with the geometry proposed for the $CuCl_6^{4-}$ complex in (3-Cl-an)$_8$[$CuCl_6$]Cl_4 was obtained using the above warping parameter and the value $S_\theta = -600$ cm^{-1}. The resulting potential surface is shown in Figure 8b, which shows that the effect of the strain is to raise one potential well significantly in energy (this corresponds to the geometry with the long Cu–Cl bond in the direction of the strain), while shifting the two essentially equivalent low-energy wells from positions corresponding to complexes of tetragonal symmetry to ones of orthorhombic geometry.

The g values of each vibronic state were calculated from the electronic part of the wave function, including spin–orbit coupling with the excited electronic states.[18] The temperature dependence of the g values of the complex as a whole was estimated by calculating the Boltzmann population distribution over the energy levels. Rapid electron exchange between the levels was assumed, which seems reasonable even at low temperatures, since the compounds are magnetically coupled (eq 3). Below ~ 10 K the **g** tensor becomes orthorhombic, this component increasing with decreasing temperature and becoming as large as $\delta g \approx 0.04$ at 4 K. The introduction of an orthorhombic strain component $S_\epsilon = 0.3$ cm^{-1} produces good agreement with these data, as may be seen from the plot shown in Figure 9 (full lines). This is of the same order of magnitude as the random strains thought to be present in all crystal lattices.[47] These random strains are considered to play an important role in Jahn–Teller systems, by acting to "lock" complexes into particular potential wells when these are otherwise equivalent. An isotropic orbital reduction parameter $k = 0.67$ was used in the calculations, similar to that

(45) Bacci, M. *Chem. Phys.* **1979**, *40*, 237.
(46) Reynolds, R. W.; Boatner, L. A.; Abraham, M.; Chen, Y. *Phys. Rev. B: Solid State* **1974**, *10*, 3802.
(47) Williams, F. I. B.; Krupka, D. C.; Breen, D.P. *Phys. Rev.* **1969**, *179*, 255.
(48) O'Brien, M. C. M. *Proc. Roy. Soc. London Ser. A* **1964**, *281*, 323.

used in the CAMMAG calculation. It may be noted that at room temperature the observed g values are slightly higher than the calculated ones. Possibly, this is due to the fact that the excited states shift to lower energy at higher temperatures (Figure 5), a feature which was not included in the calculation.

The Cu–Cl bond lengths (Å) estimated from the vibrational wave function of the lowest state agree well with those derived from the ellipsoids of thermal motion observed in the X-ray analysis (in parentheses):

$$\text{Cu–Cl(1)} \sim 2.28(2.28);\ \text{Cu–Cl(2)} \sim 2.36\ (\sim 2.37);\ \text{Cu–Cl(3)} \sim 2.86\ (\sim 2.85)$$

The above model implies that the direction of the tetragonal strain lies approximately along the a crystal axis, causing Cu–Cl(1) to be the shortest bond. Taking this as the **z**-axis, and with the orthorhombic component of the strain acting in compression approximately along the b crystal axis, the Cu–Cl(2) direction, being defined as **y**, the electronic wave function associated with the lowest state is $0.89\ (d_{z^2-y^2}) - 0.46(d_{x^2})$ (Figures 8b and 9b). The second highest level, only about 0.5 cm^{-1} higher in energy, is effectively localised in the second low-energy well, with a vibrational wave function which suggests virtually identical bond lengths, but interchanged with respect to Cl(2) and Cl(3). The electronic wave function is $0.89(d_{z^2-x^2}) + 0.46(d_{y^2})$, which differs from that of the lowest level only in the orientation of the orbital lobes. The g-anisotropy is due to the fact that while at temperatures above $\sim$10 K both levels are essentially equally populated, so that a (thermally or exchange) averaged **g** tensor is observed. At low temperature a population difference develops which causes the observed **g** tensor to shift toward that of the lower energy orientation. Provided a $|S_\theta|/\beta$ ratio similar to that for Figure 8b is used, lower values of $|S_\theta|$ and β will also fit the low temperature g values, but a significant temperature dependence on warming is then predicted, which contradicts experiment. This is illustrated by the plot shown in Figure 9 (dashed line) for the potential surface shown in Figure 8c (corresponding to $S_\theta = -150$ cm^{-1}, $\beta \approx 137$ cm^{-1}). The sensitivity of the g values to temperature is caused by the fact that at lower values of β the potential surface of each low-energy well slopes rather gently and the barrier height between them is small, so that the higher energy levels are significantly delocalized.

In general, a complex having a potential surface corresponding to a compressed tetragonal geometry [$|S_\theta|/\beta > 9$[12]] will have g values inconsistent with those observed for (3-Cl-an)$_8$[$CuCl_6$]Cl_4 since the ground state of such a system is d_{z^2} (taking **z** as the direction of the axial strain), with g_z close to the free electron value of 2 (eq 2). However, if the axial compression is only just sufficient to overcome the tendency of copper(II) to adopt a tetragonally elongated geometry ($|S_\theta| \approx 9\beta$) a potential surface with a very shallow minimum centered on a compressed tetragonal geometry may result. The energy levels are then relatively closely spaced, and of large amplitude in ϕ-space. While the electronic part of each level is predominantly d_{z^2}, it has a significant $d_{x^2-y^2}$ contribution which increases as the quantum number of the vibronic state rises. Since the latter part of the wave function causes a positive g_z shift, a significant deviation of g_z from 2 will occur at higher temperatures, when upper energy levels are thermally populated. This situation is illustrated for the potential surface of $CuCl_6^{4-}$ appropriate to the parameters $S_\theta = -375$ cm^{-1} and $\beta \approx 34$ cm^{-1} in Figure 8d. While two low-energy wells are still apparent, the barrier-height between these is below the zero-point energy of the lowest energy level. Thus the complex has a true, compressed tetragonal geometry. The above vibronic mechanism induces a g_z value in agreement with that observed experimentally for (3-Cl-an)$_8$[$CuCl_6$]Cl_4 at room temperature but predicts a temperature dependence which is in marked contrast with experiment (Figure 9 d). A behavior analogous to this latter situation was in fact observed[13] for the CuF_6^{4-} guest complex in Cu^{2+}-doped K_2ZnF_4 ($S_\theta \approx -540$ cm^{-1}, $\beta \approx 50$ cm^{-1}).

The potential surface proposed for the $CuCl_6^{4-}$ complex in (3-Cl-an)$_8$[$CuCl_6$]Cl_4 is formally quite similar to that used to describe the behavior of the $Cu(H_2O)_6^{2+}$ complexes formed when Cu^{2+} is doped into $M_2Zn(H_2O)_6(SO_4)_2$ (M = a monovalent cation),[18] though in these latter compounds the orthorhombic strain parameter is much larger, so that one of the lower wells is significantly higher in energy than the other. The smallest energy difference occurs for Cu^{2+}-doped $K_2Zn(H_2O)_6(SO_4)_2$ ($S_\theta = -1000$ cm^{-1}, $S_\epsilon = 55$ cm^{-1}, and $\beta \approx 300$ cm^{-1}). Even in this case the two higher g values have not converged at 300 K ($g_1 = 2.04$, $g_2 = 2.15$, $g_3 = 2.42$ at 4 K, and $g_1 = 2.04$, $g_2 = 2.27$, $g_3 = 2.30$ at 298 K). The $CuCl_6^{4-}$-ion in (3-Cl-an)$_8$[$CuCl_6$]Cl_4 also shows similarities to the complex $CuCl_4(H_2O)_2^{2-}$ formed when Cu^{2+} is doped into NH_4Cl at low pH.[17] Here, the strain is tetragonal and caused by the fact that H_2O is a stronger σ-donor than Cl^-. The strain is rather small ($S_\theta \approx -200$ cm^{-1}), and two equivalent low-energy minima occur. At high temperatures, thermal population of higher, delocalized vibronic levels means that the EPR spectrum is the average of the complexes in the two minima, so that a **g** tensor of tetragonal symmetry is observed ($g_1 = 2.04_5$, $g_2 = g_3 = 2.25_6$). Below $\sim$40 K the rate of exchange between the two minima becomes slow enough that the spectra of the two different orientations can be resolved ($g_1 = 2.01_9$, $g_2 = 2.18_5$, $g_3 = 2.41_0$; note that here the rate of exchange between complexes is slow, because the Cu^{2+} ions are well separated in the lattice). The $CuCl_4(H_2O)_2^{2-}$ complex also seems to have a considerably smaller warping parameter ($\beta \approx 100$ cm^{-1}) than that of the present complex, so that the potential surface is more similar to that shown in Figure 8c than Figure 8b, and g_1 shows a significant temperature dependence.

General Conclusions and Suggestions for Future Work

The EPR and electronic spectra suggest that at the local level the $CuCl_6^{4-}$ complex in (3-Cl-an)$_8$[$CuCl_6$]Cl_4 has a tetragonally elongated coordination geometry with a distinct orthorhombic component to the bonding, rather than the compressed tetragonal geometry previously proposed. The apparent tetragonal compression revealed by the X-ray crystal structure results from disorder of the intermediate and long Cu–Cl bonds of the $CuCl_6^{4-}$ units. The disorder may well be dynamic at elevated temperatures. Unfortunately, it is not possible to investigate whether a ciritical temperature exists at which a transition to statically distorted $CuCl_6^{4-}$ polyhedra occurs from the g versus T dependencies, because exchange coupling (eq 3) and temperature average the g values in the same way. The magnetic results suggest that at very low temperature 3-dimensional magnetic and elastic correlations exist, though the antiferrodistortive arrangement of the Cu–Cl bonds is probably not of a long-range type. Because the $CuCl_6^{4-}$ polyhedra are isolated in the unit cell, with rather large Cu^{2+}–Cu^{2+} separations in the (100) plane, the cooperative elastic forces are indeed expected to be rather small.

Metal–ligand bonding parameters derived from the EPR and optical spectra are in good agreement with the bond lengths derived from the thermal ellipsoids of the chloride ions assuming a disorder model.[49] The likely potential surface of the $CuCl_6^{4-}$ ion may be modeled by applying a lattice strain of tetragonal symmetry with a tiny orthorhombic component to the warped "Mexican hat" potential surface conventionally used to describe a 6-coordinate copper(II) complex. While the parameters defining this potential surface are only semiquantitative, they suggest a rather high value for the warping parameter $\beta \geq \sim 300$ cm^{-1}. The axial

(49) After preparation of this paper, the extended X-ray absorption fine structure (EXAFS) of the compound was measured. Preliminary results support the local elongated tetragonal geometry proposed in the present study, with bond lengths very similar to thiose derived from the thermal ellipsoids. Ellis, P.; Freeman, H. Private communication.

strain acting to compress the $CuCl_6^{4-}$ ion, $S_\theta \approx -600$ cm^{-1}, is similar to values reported for analogous complexes (*e.g.* S_θ lies between −550 and −1000 cm^{-1} for the $Cu(H_2O)_6^{2+}$ complex in a range of compounds[18]).

A possible way of independently verifying the nature of the strain would be to determine the crystal structure of an analogous compound formed by a non-Jahn–Teller active metal of similar size such as zinc(II) or magnesium(II). Although such an approach cannot be expected to be fullproof, it has been found[1,18] that where these are known, the distortions generally do mirror the lattice strain parameters estimated from the analysis of the temperature dependence of the **g** tensors of the corresponding copper(II) complexes. If a similar lattice strain occurs, the present results suggest that a compound of the form (3-Cl-an)$_8$[MCl_6]-Cl_4 where M = Zn or Mg should have a structure basically similar to the "averaged" structure observed for the copper(II) compound, but with axial bonds ~0.02 Å shorter than the in-plane ones. Host compounds would also provide a suitable diamagnetic host lattice for EPR studies. The slow rate of electron exchange expected for Cu^{2+} doped in such a lattice should mean that the EPR spectrum of the $CuCl_6^{4-}$ complex isolated in each potential well could be studied. We are currently investigating whether it is possible to prepare compounds of this constitution with metal ions other than copper(II).

The small anisotropy which develops in the $g_\perp$ signal of (3-Cl-an)$_8$[$CuCl_6$]Cl_4 below ~10 K may be interpreted in terms of a tiny orthorhombic component of the lattice strain, making the two alternative orientations of the $CuCl_6^{4-}$ complex slightly inequivalent in energy. This could be tested by extending the measurements below 4 K, where the model predicts a dramatic increase of the divergence between the upper two g values. However, we presently have not the experimental capability to carry out such measurements. Below ~9 K the EPR spectra also show unusual "satellite" lines, and these are ascribed to internal magnetic fields generated by the magnetic ordering in the compound. We are currently attempting a quantitative interpretation of this phenomen, and this would also be greatly assisted if spectra at temperatures below 4 K were available.

Acknowledgment. The financial assistance of the Alexander von Humboldt Foundation to M.A.H is gratefully acknowledged, and Dr. M. Gerloch of the University of Cambridge is thanked for making available the computer program CAMMAG. Dr. M. J. Riley is thanked for useful discussions.